3WCC temperature integration in a gasoline-HEV optimal energy management strategy

Pierre Michel, Alain Charlet, Guillaume Colin, Yann Chamaillard, Cédric Nouillant, Gérard Bloch

Hindawi Publishing Corporation
Advances in Mechanical Engineering
Volume 2014, Article ID 802597, 8 pages
http://dx.doi.org/10.1155/2014/802597

Research Article

3WCC Temperature Integration in a Gasoline-HEV Optimal Energy Management Strategy

Pierre Michel,[1,2] Alain Charlet,[1] Guillaume Colin,[1] Yann Chamaillard,[1] Cédric Nouillant,[2] and Gérard Bloch[3]

[1] *University of Orléans, PRISME, EA 4229, 45072 Orléans, France*
[2] *PSA Peugeot Citroën, Case courrier LG073, 92250 La Garenne Colombes, France*
[3] *Centre de Recherche en Automatique de Nancy (CRAN), Université de Lorraine, CNRS, 54519 Vandoeuvre-Lès-Nancy, France*

Correspondence should be addressed to Pierre Michel; pierre.michel@mpsa.com

Received 16 September 2013; Accepted 17 December 2013; Published 12 February 2014

Academic Editor: Yuan Zou

For a gasoline-hybrid electric vehicle (HEV), the energy management strategy (EMS) is the computation of the distribution between electric and gasoline propulsion. Until recently, the EMS objective was to minimize fuel consumption. However, decreasing fuel consumption does not directly minimize the pollutant emissions, and the 3-way catalytic converter (3WCC) must be taken into account. This paper proposes to consider the pollutant emissions in the EMS, by minimizing, with the Pontryagin minimum principle, a tradeoff between pollution and fuel consumption. The integration of the 3WCC temperature in the EMS is discussed and finally a simplification is proposed.

1. Introduction

A gasoline-electric hybrid electric vehicle (HEV) has two power sources (fuel and electricity) and two associated converters to ensure propulsion (a gasoline engine and an electrical machine), allowing stop-and-start and zero-emission vehicle operating modes. In this context, the energy management strategy (EMS), which consists in finding the best power distribution to meet a drivers request, provides the possibility of reducing the fuel consumption [1].

For this reduction, different optimal offline strategies were proposed, based on the Pontryagin minimum principle (PMP) [2] or dynamic programming derived from Bellman's principle of optimality [3]. Some suboptimal online strategies were adapted from the PMP method such as the equivalent consumption minimization strategy (ECMS) [4] or adaptive-ECMS (A-ECMS) [5].

However, decreasing the fuel consumption does not directly ensure the reduction of the pollutant emissions. In order to minimize both fuel consumption and pollutant emissions, three off-line EMS have been proposed.

(i) Strategy A. This strategy minimizes a tradeoff between engine pollutant emissions and fuel consumption with the PMP method in the same way as for fuel consumption minimization. It has been applied in diesel-HEV [6–8] and gasoline-HEV [9] contexts.

(ii) Strategy C. This strategy now minimizes a tradeoff between post-3WCC or vehicle pollutant emissions and fuel consumption. The PMP is applied by considering, as a second state, the 3-way-catalytic converter (3WCC) temperature [10–12], because of its key role in converting the engine pollution emissions.

(iii) Strategy B. This strategy is a simplification of strategy C, without the 3WCC temperature constraint.

The paper compares these three strategies with a reference strategy minimizing only the fuel consumption. It highlights the better results of strategy B compared to those of strategy C. Integrating the 3WCC temperature dynamics, as in strategy C, reduces pollutant emissions with a relatively small

increase of fuel consumption. Nevertheless, better reductions with smaller increase in fuel consumption can be found with a simpler method by changing the tradeoff between engine pollution and fuel consumption and without 3WCC temperature constraint (strategy B).

The next section describes a 4-dynamics gasoline-HEV model, determined with the aim of testing different strategies. Section 3 formalizes the reference fuel consumption minimization strategy with the PMP method and introduces strategies A, B, and C. For these strategies, the next section presents some simulation results for a first tradeoff between fuel consumption and NO_X emissions. A second tradeoff between fuel consumption, CO, and NO_X emissions is proposed. This compromise shows also good results in decreasing each pollutant species emissions including HC. Finally a conclusion is given and the simplification of strategy C into strategy B, where the 3WCC temperature dynamics is not considered explicitly in the PMP optimization method, is discussed.

2. Gasoline-HEV Model

The HEV is a parallel mild-hybrid vehicle with the electrical machine connected to the gasoline engine by a belt. The HEV is modeled with a 4-state model represented in Figure 1. The four dynamical states are the battery state of charge (SOC), 3WCC temperature θ_{cata}, engine block temperature θ_i, and engine water temperature θ_w. Other variables are static and depend directly on the driving speed. From the driving cycle speed, with the vehicle and gearbox models, the rotation speeds of the thermal engine ω_i and electrical machine ω_e and the requested torque T_0 can be deduced; see Figure 1. These computations take into account the gearbox ratio and the different transmission ratios and efficiencies.

2.1. Engine Model. The engine temperature θ_i and the water temperature θ_w dynamics are deduced from a simple 2-state zero-dimensional thermal model derived from the heat equation. A look-up table gives the used fuel mass flow rate $\dot{m}_{\text{fuel}}$ from the engine speed ω_i and torque T_i. The engine pollutant emissions $\dot{m}_{\text{eng}X}$, $X \in \{\text{CO}, \text{HC}, \text{NO}_X\}$, are also deduced from ω_i and T_i with three maps then penalized with respect to θ_i and engine restarting. Soot emissions, considered only recently for gasoline engines, are out of the scope of this paper.

2.2. 3WCC Model. In the gasoline-HEV context, the 3WCC is the only current technology that ensures that vehicles based on a spark-ignition engine comply with the CO, HC, and NO_X emission standards. The operation of a 3WCC can be expressed by its pollutant conversion efficiency, defined as

$$\eta_X = 1 - \frac{\dot{m}_{\text{veh}X}}{\dot{m}_{\text{eng}X}}, \quad X \in \{\text{CO}, \text{HC}, \text{NO}_X\}, \tag{1}$$

where $\dot{m}_{\text{eng}X}$ and $\dot{m}_{\text{veh}X}$ are the mass flow rates of pollutant species X, respectively, at the input (the *engine* emissions) and output (the *vehicle* emissions) of the 3WCC.

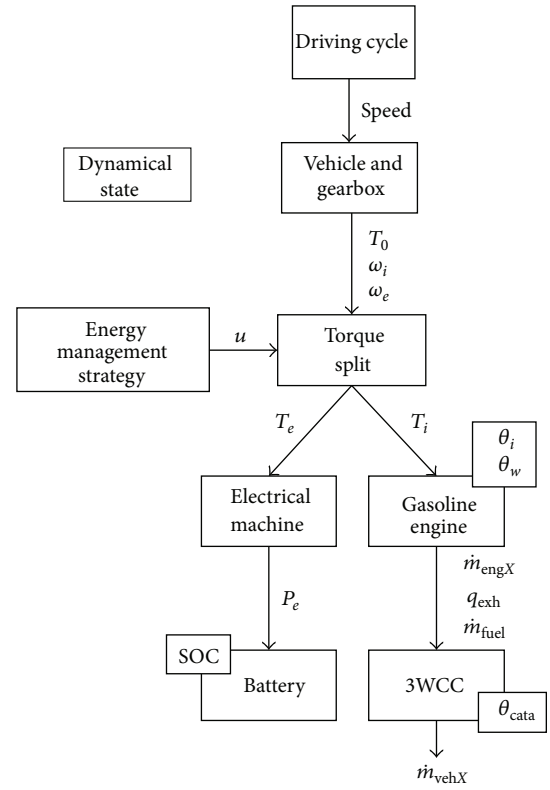

Figure 1: HEV model with four dynamical states θ_i, θ_w, SOC and θ_{cata}.

The conversion is influenced by the following variables:

(i) temperature of the 3WCC monolith, θ_{cata}, deduced from a simple 1-state zero-dimensional model,

(ii) flow rate of exhaust gas through the monolith, q_{exh}, deduced from ω_i and T_i with a map,

(iii) air-fuel ratio (AFR) of the mixture in the spark-ignition engine.

The dependence of the conversion efficiencies to AFR is neglected here, insofar as the air/fuel mixture is considered at the stoichiometry.

Equation (1) can be rewritten as

$$\dot{m}_{\text{veh}X} = (1 - \eta_X)\, \dot{m}_{\text{eng}X}. \tag{2}$$

For each pollutant, the conversion efficiency is computed from the 3WCC temperature θ_{cata} and exhaust gas flow rate q_{exh} with two maps:

$$\eta_X = \eta_{X\theta_{\text{cata}}}(\theta_{\text{cata}})\, \eta_{Xq_{\text{exh}}}(q_{\text{exh}}). \tag{3}$$

2.3. Battery Model. At each time t, the power delivered by the electric machine P_e is computed from the speed ω_e and torque T_e:

$$P_e = \omega_e T_e. \tag{4}$$

Then, the electrochemical battery power P_χ is written from the power balance:

$$P_\chi = -P_e - P_{\text{los}} - P_{\text{aux}}, \tag{5}$$

where the power losses P_{los} are deduced from the speed ω_e and torque T_e by a look-up table and the power used by the auxiliaries P_{aux} is considered constant here.

From (5), using an internal resistance model for the battery, the battery voltage U_{bat} can be deduced as

$$U_{\text{bat}} = \frac{U_0}{2} + \sqrt{\frac{U_0^2}{4} - \frac{P_\chi}{R_{\text{int}}}}, \tag{6}$$

where U_0 is the open circuit voltage and R_{int} the internal resistance deduced from SOC by two look-up tables.

Finally, by using (5) and (6), the battery current intensity

$$I_{\text{bat}} = \frac{P_\chi}{U_{\text{bat}}} \tag{7}$$

leads to the SOC dynamics

$$\dot{\text{SOC}} = c\frac{I_{\text{bat}}}{Q_{\max}}, \tag{8}$$

where $Q_{\max}$ is the battery capacity and c is a constant allowing to obtain a dimensionless expression of SOC in %.

2.4. Control Model. A parallel HEV has two propulsion systems and the requested torque at the entrance of the gearbox T_0 is simply

$$T_0 = T_i + T_e, \tag{9}$$

where the thermal engine torque T_i and electrical machine torque T_e take into account the different transmission ratios to be expressed in the same referential, the entrance of the gearbox.

A torque split variable u is introduced as the ratio between the electrical machine torque and the requested torque:

$$u = \frac{T_e}{T_0}. \tag{10}$$

Note that many variables can be now noted with respect to torque split control variable u, as, for example, the engine $\dot{m}_{\text{eng}X}(u)$ or vehicle $\dot{m}_{\text{veh}X}(u)$ emissions.

The goal of the EMS is to find the control u that fulfills different objectives. While minimizing HEV fuel consumption is the main objective, other secondary objectives can be considered such as oil temperature maximization [13] (to reduce fuel consumption), drivability [14], limitation of battery aging [15] or, as in this paper, reduction of pollutant emissions [10–12].

3. Optimal Strategies

Some recalls of the optimization framework are given first. Then the strategies are presented for fuel consumption minimization, and next for pollution/fuel consumption joint minimization, where a simplification is proposed.

3.1. Pontryagin Minimum Principle. Consider a problem P_0 where the goal is to minimize a discrete-time cost function $J(\mathbf{x}(t), \mathbf{u}(t))$, where $\mathbf{x}(t)$ is the state vector and $\mathbf{u}(t)$ the control vector. The system is expressed by the state vector dynamics:

$$\dot{\mathbf{x}}(t) = f(\mathbf{x}(t), \mathbf{u}(t)) \tag{11}$$

and the criterion to be minimized is expressed by

$$J(\mathbf{x}(t), \mathbf{u}(t)) = \Phi\left(\mathbf{x}\left(t_f\right)\right) + \int_{t_0}^{t_f} L(\mathbf{x}(t), \mathbf{u}(t))\, dt, \tag{12}$$

where $\Phi(\mathbf{x}(t_f))$ is the final state constraint at final time t_f and $L(\mathbf{x}(t), \mathbf{u}(t))$ is a cost function. With an initial constraint

$$\mathbf{x}\left(t_0\right) = x_0, \tag{13}$$

P_0 can be written, with U the admissible control space, as

$$P_0 : \begin{cases} \min\limits_{u \in U} J(\mathbf{x}(t), \mathbf{u}(t)), & t \in \left[t_0, t_f\right], \\ \dot{\mathbf{x}}(t) = f(\mathbf{x}(t), \mathbf{u}(t)), \\ \mathbf{x}\left(t_0\right) = x_0. \end{cases} \tag{14}$$

Introducing the Hamiltonian

$$H(\mathbf{x}(t), \mathbf{u}(t), \boldsymbol{\lambda}(t)) = L(\mathbf{x}(t), \mathbf{u}(t)) + \boldsymbol{\lambda}^T(t) f(\mathbf{x}(t), \mathbf{u}(t)), \tag{15}$$

with the Lagrange parameter vector (or costate) $\boldsymbol{\lambda}(t)$, P_0 can be rewritten as a dual problem P_O':

$$P_O' \begin{cases} \dot{\mathbf{x}}(t) = f(\mathbf{x}(t), \mathbf{u}(t)), \\ \mathbf{x}\left(t_0\right) = x_0, \\ \dot{\boldsymbol{\lambda}}^T(t) = -\dfrac{\partial H(\mathbf{x}(t), \mathbf{u}(t), \boldsymbol{\lambda}(t), t)}{\partial \mathbf{x}}, \\ \dot{\boldsymbol{\lambda}}^T\left(t_f\right) = \dfrac{\partial \phi\left(\mathbf{x}\left(t_f\right)\right)}{\partial \mathbf{x}\left(t_f\right)}, \\ \mathbf{u}^*(t) = \underset{u \in U}{\operatorname{argmin}} H(\mathbf{x}(t), \mathbf{u}(t), \boldsymbol{\lambda}(t)). \end{cases} \tag{16}$$

The last equation, where $\mathbf{u}^*(t)$ is the optimal control minimizing (12), corresponds to the Pontryagin minimum principle (PMP) [2].

3.2. Fuel Consumption Minimization Strategy. Optimal (offline) strategies assume the knowledge of the full driving horizon, from time t_0 to time t_f. Then, for fuel consumption, the following performance index has to be minimized:

$$J_{\text{fuel}} = \Phi\left(\text{SOC}\left(t_f\right)\right) + \int_{t_0}^{t_f} \dot{m}_{\text{fuel}}(u)\, dt, \tag{17}$$

where $\dot{m}_{\text{fuel}}(u)$ is the engine fuel mass flow rate and $\Phi(\text{SOC}(t_f))$ is a final state constraint ensuring charge sustaining:

$$\Phi\left(\text{SOC}\left(t_f\right)\right) = \begin{cases} 0, & \text{if SOC}\left(t_f\right) = \text{SOC}\left(t_0\right), \\ \infty, & \text{else.} \end{cases} \quad (18)$$

The performance index (17) is minimized with PMP, as described above, considering the one-state SOC dynamics (7):

$$\dot{\text{SOC}} = f\left(\text{SOC}, u\right). \quad (19)$$

To this end, the Hamiltonian

$$H\left(\text{SOC}, u, \lambda, t\right) = \dot{m}_{\text{fuel}}\left(u\right) + \lambda \dot{\text{SOC}} \quad (20)$$

is defined, where λ is the co-state associated with the SOC dynamics, respecting

$$\dot{\lambda} = -\frac{\partial H\left(\text{SOC}, u, \lambda, t\right)}{\partial \text{SOC}}. \quad (21)$$

The optimal control u^* is obtained by minimizing (20), at each time t:

$$u^* = \underset{u \in U}{\operatorname{argmin}}\, H\left(\text{SOC}, u, \lambda, t\right). \quad (22)$$

In the case of HEV, considering

$$\frac{\partial H\left(\text{SOC}, u, \lambda, t\right)}{\partial \text{SOC}} = 0 \quad (23)$$

has a very little influence on fuel consumption, since the SOC dependence on R_{int} and U_0 is low. Then $\dot{\lambda} = 0$, λ is considered constant, and a simple binary search can find the value ensuring the HEV fuel consumption minimization and charge sustaining. Note, however, that this value strongly depends on the considered cycle [1].

3.3. Pollution Constrained Fuel Consumption Minimization Strategies

Strategy A. The first approach, when considering pollution in the EMS, is to define a tradeoff $\dot{m}_{\text{eng}}(u)$ between fuel consumption and *engine* pollutant emissions:

$$\dot{m}_{\text{eng}}\left(u\right) = \left(1 - \sum_X \alpha_X\right) \dot{m}_{\text{fuel}}\left(u\right) + \sum_X \alpha_X \dot{m}_{\text{eng}X}\left(u\right), \quad (24)$$

where $\dot{m}_{\text{eng}X}$ are the mass flow rates of engine pollutant species X, $X \in \{\text{CO}, \text{HC}, \text{NO}_X\}$, and α_X are the corresponding weighting factors, and derive a new performance index

$$J_{\text{eng}} = \Phi\left(\text{SOC}\left(t_f\right)\right) + \int_{t_0}^{t_f} \dot{m}_{\text{eng}}\left(u\right) dt \quad (25)$$

that can be minimized as (17).

Strategy C. The second approach is based on the tradeoff $\dot{m}_{\text{veh}}(u)$ between fuel consumption and *vehicle* pollutant emissions

$$\dot{m}_{\text{veh}}\left(u\right) = \left(1 - \sum \alpha_X\right) \dot{m}_{\text{fuel}}\left(u\right) + \sum \alpha_X \dot{m}_{\text{veh}X}\left(u\right). \quad (26)$$

In (3), for the minimization, the 3WCC conversion efficiencies are simplified as

$$\eta_X = f\left(\theta_{\text{cata}}\right). \quad (27)$$

A new performance index

$$J_{\text{veh}} = \Phi\left(\text{SOC}\left(t_f\right)\right) + \int_{t_0}^{t_f} \dot{m}_{\text{veh}}\left(u\right) dt \quad (28)$$

is then defined. If the θ_{cata} dynamics is considered during minimization, the Hamiltonian becomes:

$$H\left(\text{SOC}, \theta_{\text{cata}}, u, \boldsymbol{\lambda}, t\right) = \dot{m}_{\text{veh}}\left(u\right) + \lambda_1 \dot{\text{SOC}} + \lambda_2 \dot{\theta}_{\text{cata}}. \quad (29)$$

Using (23), the first co-state λ_1 can be found constant as in the fuel consumption minimization strategy. The second co-state λ_2 associated with the 3WCC temperature dynamics is obtained by solving

$$\dot{\lambda}_2 = -\frac{\partial H\left(\text{SOC}, \theta_{\text{cata}}, u, \boldsymbol{\lambda}, t\right)}{\partial \theta_{\text{cata}}}, \quad (30)$$

yielding the exponential form

$$\lambda_2\left(t\right) = \lambda_{20} e^{at - b(u,t)}, \quad (31)$$

where a is a constant and b is a function, which can be found from (26) and (27), and λ_{20} is the second co-state initial condition.

Strategy B. This strategy is a simplification of strategy C and considers a zero 3WCC temperature co-state in (31):

$$\lambda_{20} = \lambda_2\left(t\right) = 0. \quad (32)$$

The idea is to take into account in the minimization strategy the 3WCC temperature dynamics only through the vehicle pollutant emissions (26) and not in (29).

4. Results

This section presents some simulation results obtained on Worldwide harmonized Light vehicles Test Cycles (WLTC). Tradeoffs between fuel consumption and NO_X emissions, then CO/NO_X emissions, are minimized with the strategies presented above, which are compared.

Fuel consumption minimization strategy is the reference and the corresponding fuel consumption and pollutant emissions are obtained with instantaneous minimization of the Hamiltonian (20). The constant value of λ is found by a binary search while respecting the final SOC constraint (18).

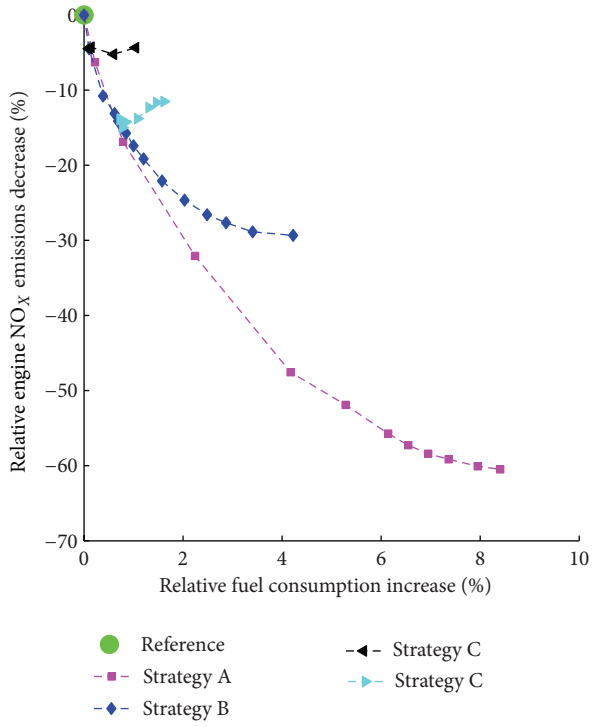

FIGURE 2: Relative NO_X engine emissions reduction versus relative fuel consumption increase.

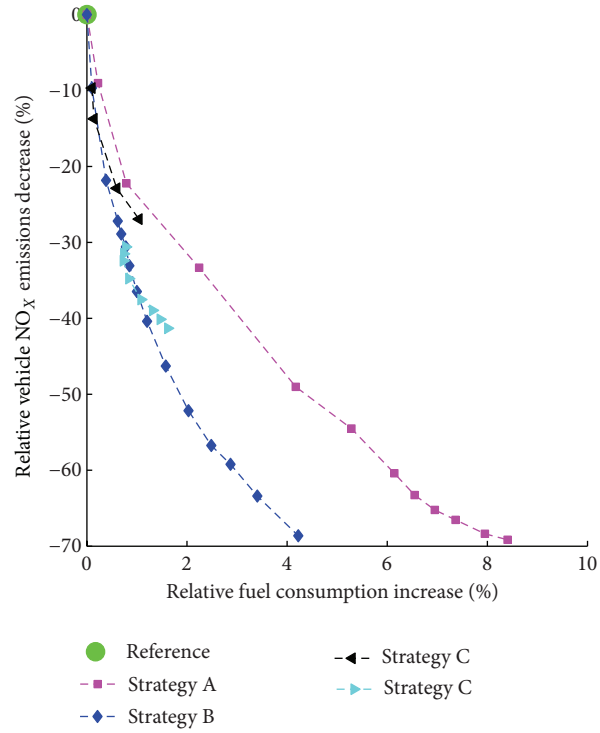

FIGURE 3: Relative NO_X vehicle emissions reduction versus relative fuel consumption increase.

4.1. NO_X Emissions/Fuel Consumption Compromise. Tradeoffs between NO_X emissions and fuel consumption are chosen and minimized with different strategies.

The first tradeoffs between *engine* NO_X emissions and fuel consumption

$$\dot{m}_{\text{eng}}(u) = \left(1 - \alpha_{NO_X}\right)\dot{m}_{\text{fuel}}(u) + \alpha_{NO_X}\dot{m}_{\text{engNO}_X}(u) \quad (33)$$

are minimized with strategy A, for different values of α_{NO_X}, from $\alpha_{NO_X} = 0$, which is the reference, to the maximal value allowed by the battery size. Note that the maximal battery demand translates into the maximum SOC deviation obtained during an optimal simulation.

Next, tradeoffs between *vehicle* NO_X emissions and fuel consumption

$$\dot{m}_{\text{veh}}(u) = \left(1 - \alpha_{NO_X}\right)\dot{m}_{\text{fuel}}(u) + \alpha_{NO_X}\dot{m}_{\text{vehNO}_X}(u) \quad (34)$$

are minimized with strategies B and C.

For strategy B, the results are obtained by minimizing a Hamiltonian such as (29) for different α_{NO_X} values in (34) and a choice of $\lambda_{20} = 0$ as in (32). For strategy C, the results are obtained for two fixed α_{NO_X} values in (34) and different values of λ_{20} in (31).

The results presented in Figure 2 show that strategy A yields the largest reductions in engine pollution for the lowest increases in fuel consumption. As expected, strategy A is the best one to minimize the *engine* NO_X emissions.

Figure 3 shows that strategy B and strategy C are more efficient in minimizing the *vehicle* NO_X emissions. At a fixed tradeoff between NO_X vehicle pollution and fuel consumption $\dot{m}_{\text{veh}}(u)$ as defined in (34) a judicious choice of λ_{20} in strategy C can reduce the NO_X vehicle emissions [10–12]. However, strategy B can lead to better results provided that a good choice of α_{NO_X} has been made in $\dot{m}_{\text{veh}}(u)$ and a zero 3WCC temperature co-state has been chosen.

Next, Figure 4 reveals that strategy C implies a stronger use of the battery than strategy B, which is not desirable. The battery demands are represented by the maximum SOC deviation obtained during a driving cycle with the optimal control.

Figure 5 shows the trajectories of SOC, relative 3WCC temperature θ_{cata}, and relative cumulative normalized NO_X *engine* emissions $\dot{m}_{\text{engNO}_X}$ and *vehicle* emissions $\dot{m}_{\text{vehNO}_X}$ for strategies A and B. The parameters have been chosen to ensure the same fuel consumption decrease. The 3WCC conversion consideration by strategy B ensures a better NO_X conversion than strategy C with the same level of battery solicitations.

4.2. CO/NO_X Emissions/Fuel Consumption Compromise. Similar to (33) and (34), tradeoffs between CO and NO_X engine emissions and fuel consumption, with $\alpha_{\text{CO}} = \alpha_{NO_X}$ and

$$\begin{aligned}\dot{m}_{\text{eng}}&(u(t), t)\\ &= \left(1 - \alpha_{\text{CO}} - \alpha_{NO_X}\right)\dot{m}_{\text{fuel}}(u)\\ &\quad + \alpha_{\text{CO}}\dot{m}_{\text{engCO}}(u) + \alpha_{NO_X}\dot{m}_{\text{engNO}_X}(u),\end{aligned} \quad (35)$$

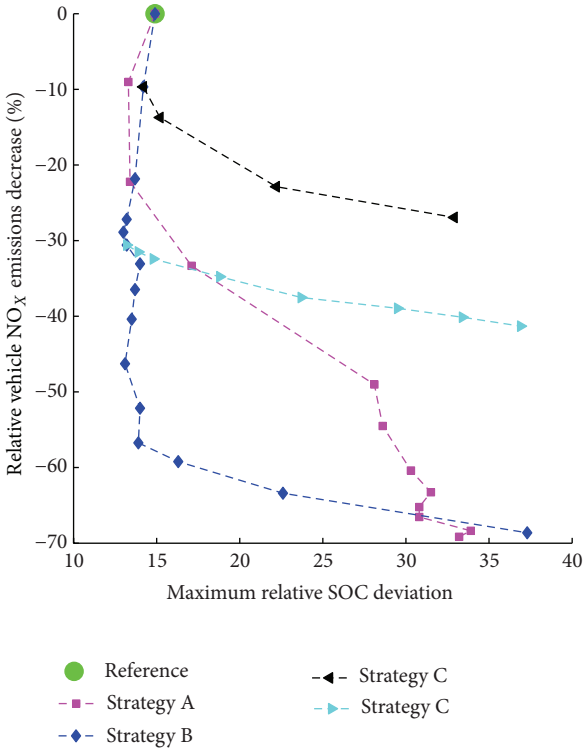

FIGURE 4: Relative NO_X vehicle emissions reduction versus maximum relative SOC deviation (zero costate).

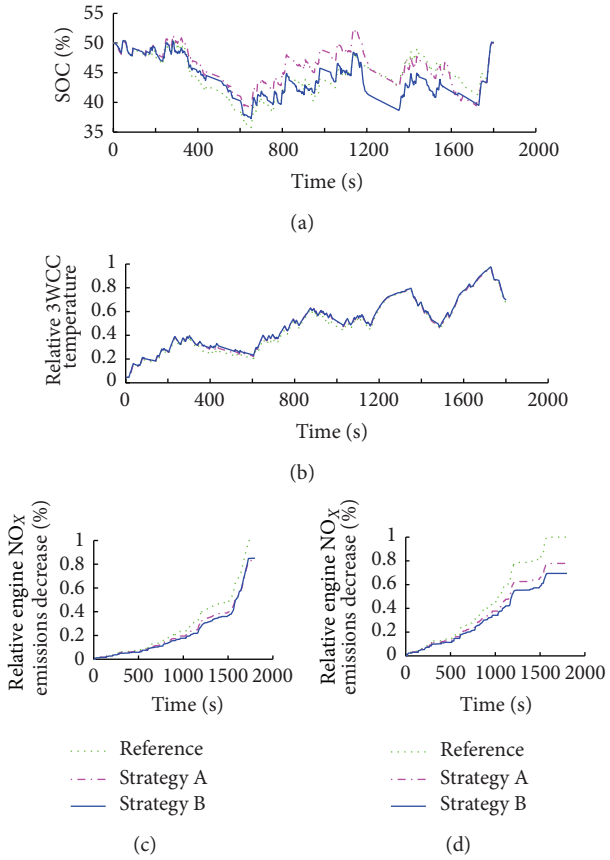

FIGURE 5: SOC, 3WCC temperature, and NO_X engine and vehicle emissions trajectories.

are minimized with strategy A, and tradeoffs between CO and NO_X vehicle emissions and fuel consumption, with $\alpha_{CO} = \alpha_{NO_X}$ and

$$\begin{aligned} &\dot{m}_{veh}(u) \\ &= \left(1 - \alpha_{NO_X} - \alpha_{CO}\right) \dot{m}_{fuel}(u) \\ &\quad + \alpha_{CO} \dot{m}_{vehCO}(u) + \alpha_{NO_X} \dot{m}_{vehNO_X}(u), \end{aligned} \tag{36}$$

are minimized with strategies B and C.

For the three strategies, the vehicle emissions with respect to fuel consumption are shown in Figure 6, for HC, Figure 7, for NO_X, and Figure 8, for CO.

Again, strategies B and C are better than strategy A in minimizing vehicle emissions, and, compared to strategy C, strategy B leads to better reduction of vehicle pollutant emissions, including HC.

Note that other compromises can be easily built with different objectives concerning CO, NO_X, and/or HC pollutants.

5. Conclusion

Optimal strategies have been proposed to minimize fuel consumption while taking pollutant emissions into consideration. A simple tradeoff between *engine* pollution and fuel consumption can be minimized with the PMP, ensuring good results.

These results can be improved if the strategy takes the 3WCC behavior into account. Two ways are proposed to

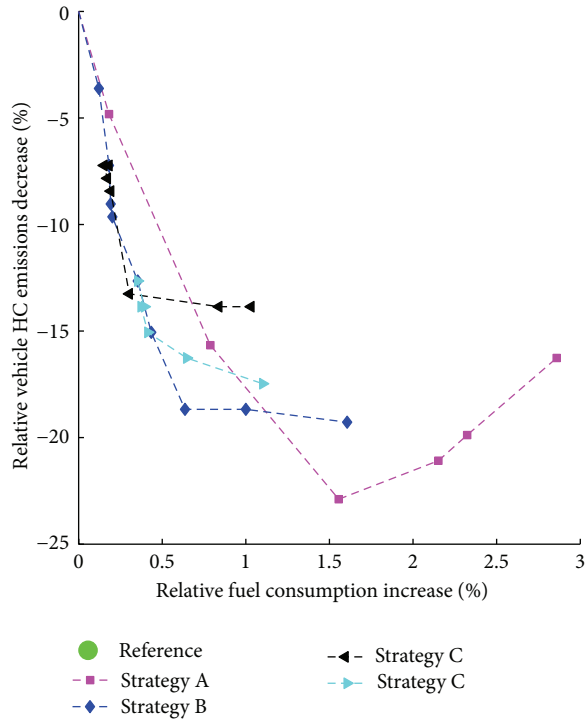

FIGURE 6: Relative HC vehicle emissions reduction versus relative fuel consumption increase.

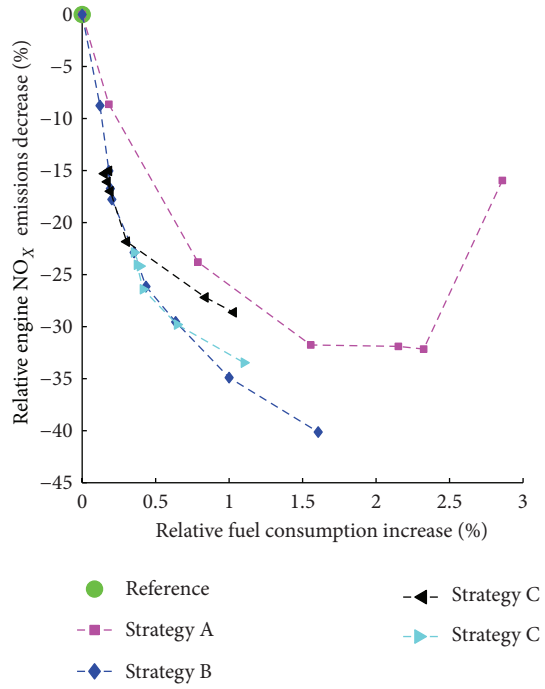

Figure 7: Relative NO_X vehicle emissions reduction versus relative fuel consumption increase.

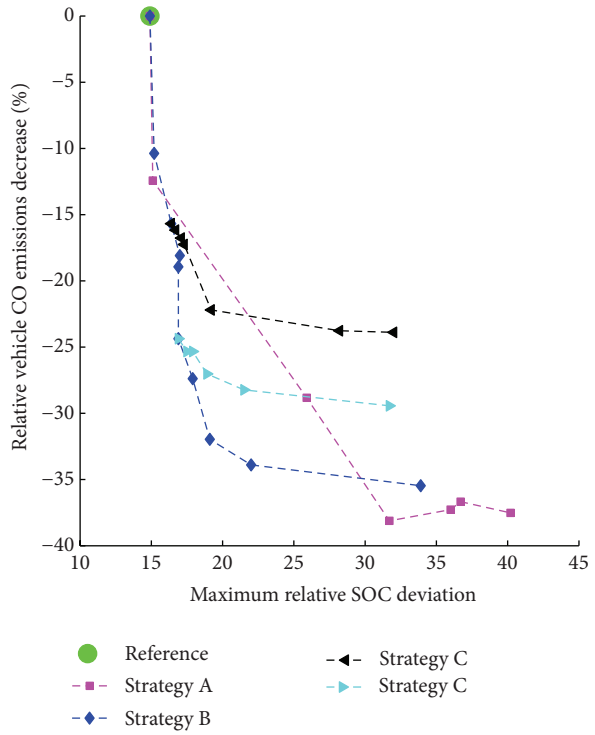

Figure 8: Relative CO vehicle emissions reduction versus relative fuel consumption increase.

minimize a tradeoff between vehicle pollution and fuel consumption. The first one includes the 3WCC temperature dynamics in the Hamiltonian (strategy C), while the second one does not include this dynamics (strategy B). Introducing a second dynamics improves the results, but better results are found with lower battery demands with a zero second co-state, simply by changing the compromise between vehicle pollution and fuel consumption.

To conclude, the fuel consumption minimization with pollution constraint does not require considering directly the 3WCC temperature in the minimization method, as in strategy C. The simplicity and better results of strategy B are preferable for a future on-line adaptation. This is reinforced by the frequent difficulties in deducing the 3WCC temperature and its associated co-state in a real environment.

Conflict of Interests

The authors declare that there is no conflict of interests regarding the publication of this paper.

References

[1] L. Guzzella and A. Sciarretta, *Vehicle Propulsion Systems*, Springer, 2007.

[2] L. S. Pontryagin, V. G. Boltyanskii, R. V. Gamkrelidze, and E. F. Mishechenko, *The Mathematical Theory of Optimal Processes*, John Wiley & Sons, 1962.

[3] R. Bellman, "Dynamic programming and the smoothing problem," *Management Science*, vol. 3, no. 1, pp. 111–113, 1956.

[4] G. Paganelli, S. Delprat, T. M. Guerra, J. Rimaux, and J. J. Santin, "Equivalent consumption minimization strategy for parallel hybrid powertrains," in *Proceedings of the 55th Vehicular Technology Conference*, vol. 4, pp. 2076–2081, May 2002.

[5] C. Musardo, G. Rizzoni, and B. Staccia, "A-ECMS: an adaptive algorithm for hybrid electric vehicle energy management," in *Proceedings of the 44th IEEE Conference on Decision and Control, and the European Control Conference (CDC-ECC '05)*, pp. 1816–1823, December 2005.

[6] O. Grondin, L. Thibault, P. Moulin, A. Chasse, and A. Sciarretta, "Energy management strategy for diesel hybrid electric vehicle," in *Proceedings of the 7th IEEE Vehicle Power and Propulsion Conference (VPPC '11)*, September 2011.

[7] F. Millo, L. Rolando, and E. Servetto, "Development of a control strategy for complex light-duty Diesel-Hybrid powertrains," SAE Technical Paper 2011-24-0076, 2011.

[8] C. Musardo, B. Staccia, S. Midlam-Mohler, Y. Guezennec, and G. Rizzoni, "Supervisory control for NO_x reduction of an HEV with a mixed-mode HCCI/CIDI engine," in *Proceedings of the American Control Conference (ACC '05)*, vol. 6, pp. 3877–3881, June 2005.

[9] P. Michel, A. Charlet, G. Colin, Y. Chamaillard, and C. Nouillant, "Influence de l'hybridation d'un véhicule essence sur les émissions polluantes," in *Proceedings of the Conférence Internationale Francophone d'Automatique (CIFA '12)*, pp. 388–393, 2012.

[10] L. Serrao, A. Sciarretta, O. Grondin et al., "Open issues in supervisory control of hybrid electric vehicles: a unified approach using optimal control methods," *Oil & Gas Science and Technology*, vol. 69, pp. 23–33, 2011.

[11] A. Chasse, G. Corde, A. del Mastro, and F. Perez, "Online optimal control of a parallel hybrid with after-treatment constraint integration," in *Proceedings of the IEEE Vehicle Power and Propulsion Conference (VPPC '10)*, September 2010.

[12] P. Michel, A. Charlet, G. Colin, Y. Chamaillard, C. Nouillant, and G. Bloch, "Energy management of HEV to optimize fuel consumption and pollutant emissions," in *Proceedings of the 11th International Symposium on Advanced Vehicle Control*, 2012.

[13] J. Lescot, A. Sciarretta, Y. Chamaillard, and A. Charlet, "On the integration of optimal energy management and thermal management of hybrid electric vehicles," in *Proceedings of the IEEE Vehicle Power and Propulsion Conference (VPPC '10)*, September 2010.

[14] M. Debert, T. M. Padovani, G. Colin, Y. Chamaillard, and L. Guzzella, "Implementation of comfort constraints in dynamic programming for hybrid vehicle energy management," *International Journal of Vehicle Design*, vol. 58, no. 2, pp. 367–386, 2012.

[15] T. M. Padovani, M. Debert, G. Colin, and Y. Chamaillard, "Optimal energy management strategy including battery health through thermal management for hybrid vehicles," in *Proceedings of the 7th IFAC Symposium on Advances in Automotive Control*, pp. 384–389, 2013.